

Marquette University
e-Publications@Marquette

Biomedical Sciences Faculty Research and
Publications

Biomedical Sciences, Department of

9-1-2010

Molecular Requirements for Ethanol Differential Allosteric Modulation of Ligand-Gated Ion Channels Based on Selective G Beta Gamma Modulation

Gonzalo E. Yevenes
University of Concepcion

Gustavo Moraga-Cid
University of Concepcion

Ariel Avila
University of Concepcion

Leonardo Guzman
University of Concepcion

Maximiliano Figueroa
University of Concepcion

See next page for additional authors

Accepted version. *Journal of Biological Chemistry*, Vol. 285, No. 39 (September 2010): 30203-30213.
DOI. © 2010 American Society for Biochemistry and Molecular Biology. Used with permission.

Authors

Gonzalo E. Yevenes, Gustavo Moraga-Cid, Ariel Avila, Leonardo Guzman, Maximiliano Figueroa, Robert W. Peoples, and Luis G. Aguayo

Molecular Requirements for Ethanol Differential Allosteric Modulation of Glycine Receptors Based on Selective G β γ Modulation

Gonzalo E. Yevenes

*Laboratory of Neurophysiology, Department of Physiology,
University of Concepción
Concepción, Chile*

Gustavo Moraga-Cid

*Laboratory of Neurophysiology, Department of Physiology,
University of Concepción
Concepción, Chile*

Ariel Avila

*Laboratory of Neurophysiology, Department of Physiology,
University of Concepción
Concepción, Chile*

Leonardo Guzman

*Laboratory of Neurophysiology, Department of Physiology,
University of Concepción
Concepción, Chile*

Maximiliano Figueroa

*Department of Biochemistry and Molecular Biology
University of Concepción
Concepción, Chile*

Robert W. Peoples

*Department of Biomedical Sciences, Marquette University
Milwaukee, WI*

Luis G. Aguayo

*Laboratory of Neurophysiology, Department of Physiology,
University of Concepción
Concepción, Chile*

Abstract: It is now believed that the allosteric modulation produced by ethanol in glycine receptors (GlyRs) depends on alcohol binding to discrete sites within the protein structure. Thus, the differential ethanol sensitivity of diverse GlyR isoforms and mutants was explained by the presence of specific residues in putative alcohol pockets. Here, we demonstrate that ethanol sensitivity in two ligand-gated ion receptor members, the GlyR adult α_1 and embryonic α_2 subunits, can be modified through selective mutations that rescued or impaired G $\beta\gamma$ modulation. Even though both isoforms were able to physically interact with G $\beta\gamma$, only the α_1 GlyR was functionally modulated by G $\beta\gamma$ and pharmacological ethanol concentrations. Remarkably, the simultaneous switching of two transmembrane and a single extracellular residue in α_2 GlyRs was enough to generate GlyRs modulated by G $\beta\gamma$ and low ethanol concentrations. Interestingly, although we found that these TM residues were different to those in the alcohol binding site, the extracellular residue was recently implicated in conformational changes important to generate a pre-open-activated state that precedes ion channel gating. Thus, these results support the idea that the differential ethanol sensitivity of these two GlyR isoforms rests on conformational changes in transmembrane and extracellular residues within the ion channel structure rather than in differences in alcohol binding pockets. Our results describe the molecular basis for the differential ethanol sensitivity of two ligand-gated ion receptor members based on selective G $\beta\gamma$ modulation and provide a new mechanistic framework for allosteric modulations of abuse drugs.

Keywords: Alcohol, G Proteins, Ion Channels, Receptor Regulation, Signal Transduction, Glycine Receptor, Ligand-gated Ion Channels

Introduction

Glycine receptors (GlyRs)⁴ are members of the ligand-gated ion receptor (LGIC) superfamily, which includes the Cys-loop family composed of the inhibitory γ -aminobutyric acid receptors and GlyRs and the excitatory nicotinic acetylcholine (nAChR) and 5-hydroxytryptamine receptors. These ionotropic receptors mediate fast synaptic transmission in the central nervous system (1, 2). Specifically, inhibitory GlyRs are critical for the control of excitability in the mammalian spinal cord and brain stem, regulating important physiological functions such as pain transmission, respiratory rhythms, motor coordination, and neuronal development (3,-7).

Like all Cys-loop receptors, GlyRs are heteropentameric complexes composed of α and β subunits, which can assemble to form homomeric (5α) or heteromeric ($2\alpha 3\beta$) channels. To date, molecular cloning studies have demonstrated four isoforms of the α GlyRs (α_{1-4}) and one β isoform. Homomeric and heteromeric receptors share most of the GlyR general features, including a high percentage of identity between α GlyRs ($\approx 75\%$). Nevertheless, biochemical, immunocytochemical, and *in situ* hybridization studies have shown that the expression of the subunits are developmentally and regionally regulated (3, 4, 8). For example, the α_1 subunit expression increases after birth, whereas expression of the α_2 subunit appears mainly restricted to early developmental stages (3, 4, 8, 9). On the other hand, several studies have shown that α GlyR isoforms differ in physiological properties, such as conductance, apparent agonist affinity, desensitization, and channel kinetics (3, 4, 10, 11). For instance, single-channel studies showed that the opening probability of α_2 GlyRs was very low after a fast application of glycine, suggesting that they cannot be activated by fast neurotransmitter release at synapses (11). Similarly, other electrophysiological studies have reported that α GlyR isoforms possess different sensitivities to allosteric regulators, such as neurosteroids, zinc ions, and ethanol (12,-14). These studies, in agreement with others in cultured spinal

neurons and hypoglossal motoneuron slices (15–16), showed that receptors comprising α_1 are more sensitive to ethanol than those containing α_2 subunits (12). Interestingly, this differential ethanol sensitivity was associated to alanine 52 in α_1 GlyRs, as its replacement by its α_2 GlyR counterpart (threonine or serine) generated GlyRs with a lower ethanol sensitivity (12, 17). Based on these results and other studies with cysteine-modifying reagents (18), a pocket site for ethanol was suggested to exist near the extracellular loop 2 and Ala-52 residue in α_1 GlyRs.

Despite the existence of studies that investigated several aspects of GlyR subunit functions, our knowledge on intracellular signaling that might regulate these isoforms is limited. In this context, recent evidence reveals that the α_1 GlyRs are modulated by G proteins through the G $\beta\gamma$ heterodimer (19). Noteworthy, it has recently been shown that the degree of GlyR-G $\beta\gamma$ functional interaction is critical for ethanol-induced potentiation on the glycine-activated current (20). However, it is currently unknown if G $\beta\gamma$ can bind and allosterically modulate other GlyR isoforms and if this can impact on their differential ethanol sensitivity.

In the present study we identified extracellular and transmembrane residues that control the G $\beta\gamma$ and ethanol modulation of α_1 and α_2 GlyRs. Our results show that despite both being capable of binding G $\beta\gamma$, only α_1 GlyRs were positively modulated by G $\beta\gamma$ and pharmacological ethanol concentrations. Remarkably, simultaneous switching of two residues in transmembrane domains 2 and 3 (TM2 and TM3) plus an extracellular amino acid localized in loop 2 can reversibly control the G $\beta\gamma$ modulation, generating receptors with high and low ethanol sensitivity, respectively. These results provide novel information about the relevance of G $\beta\gamma$ modulation and on the molecular basis for the differential sensitivity of LGICs to ethanol.

Experimental Procedures

cDNA Constructs

Mutations were inserted using the QuikChange™ site-directed mutagenesis kit (Stratagene) in cDNA constructs encoding the rat GlyRs in a pCI vector (Promega). For the construction of chimeric receptors, an XbaI site was added in a conserved region within the TM3 domain, allowing us to combine DNA regions by standard subcloning. All the constructions were confirmed by full sequencing. The glycine receptor amino acids were numbered according to their position in the mature protein sequence. The cDNA encoding glycine receptor subunits with a C-terminal hexahistidyl tag (His tag) were constructed using the pcDNA3.1 Directional-TOPO kit (Invitrogen), according to the manufacturer protocol. G protein β_1 -FLAG and G protein γ_2 were purchased from UMR cDNA resource center.

Cell Culture and Transfection

HEK 293 cells were cultured using standard methodologies. HEK 293 cells were transfected using Lipofectamine 2000 (Invitrogen) with 2 μ g of DNA for each plasmid studied per well. Expression of GFP was used as a marker of positively transfected cells, and recordings were made after 18–36 h. Cultured spinal neurons were prepared as described (15, 19). The recordings were performed between 5 and 14 days *in vitro*, the time in which the neurons switch the expression from α_2 GlyRs to $\alpha_1\beta$ GlyRs (4, 8, 15).

Electrophysiology

Whole-cell recordings were performed as previously described (19, 20). A holding potential of -60 mV was used. Patch electrodes were filled with 140 mM CsCl, 10 mM BAPTA, 10 mM HEPES (pH 7.4), 4 mM MgCl₂, 2 mM ATP, and 0.5 mM GTP. The external solution contained 150 mM NaCl, 10 mM KCl, 2.0 mM CaCl₂, 1.0 mM MgCl₂, 10 mM HEPES (pH 7.4), and 10 mM glucose. For G protein activation experiments, GTP γ S (0.5 mM, Sigma) was added directly to the internal solution, replacing GTP. The amplitude of the glycine current

was assayed using a brief (1–6 s) pulse of glycine every 60 s. The modulation of the glycine current by ethanol (Sigma) was assayed using a pulse of glycine (EC_{10}) co-applied with ethanol to each receptor studied, without any pre-application. In all the experiments, a brief pulse of 1 mM glycine was performed at the end of the recording period to test that the glycine concentration corresponded to the actual EC_{10} in each single experiment. Cells that displayed responses $<EC_5$ or $>EC_{15}$ were discarded. For the $G\beta\gamma$ -induced tonic modulation, human $G\beta_1$ and $G\gamma_2$ expression plasmids were cotransfected with the respective GlyR. To identify successfully transfected cells and reduce the expression variability of the $G\beta_1\gamma_2$ dimers, a pIRES2-EGFP- $G\beta_1$ plasmid was used as a positive marker. Strychnine (1 μ M) blocked all the current elicited by wild type, chimeric, and mutant glycine receptors. The methodology for single channel recordings in outside-out configuration has been previously published (19,–21). Briefly, patch pipettes were coated with R6101 elastomer (Dow-Corning) and had tip resistances of 7–15 megaohms after fire polishing. Cells were voltage-clamped at –50 mV, and the data were filtered (1-kHz low-pass 8-pole Butterworth) and acquired at 5–20 kHz using pClamp software (Axon Instruments, Inc.). Agonist and alcohol solutions were applied to cells using a stepper motor-driven rapid solution exchanger (Fast-Step, Warner Instrument Corp.) Cells were maintained in extracellular medium containing 150 mM NaCl, 5 KCl, 2 mM $CaCl_2$, 10 mM HEPES, 10 mM glucose (pH 7.4). The intracellular recording solution contained 140 mM CsCl, 2 mM Mg-ATP, 10 mM BAPTA, and 10 mM HEPES (pH 7.2).

Construction of Glutathione S-Transferase Fusion Proteins and GST Pulldown Assays

DNA fragments encoding wild type α GlyR intracellular loops were first subcloned in the GST fusion vector pGEX-5X3 (GE Healthcare). Then, GST fusion proteins were generated in *Escherichia coli* BL21 using 10 mM isopropyl 1-thio- β -D-galactopyranoside. After 6 h the cells were collected and sonicated in lysis buffer (1 \times phosphate buffer, 1% Triton X-100, and protease inhibitor mixture set II (Calbiochem)). Subsequently, proteins were purified using a glutathione resin (Novagen), and normalized amounts of GST fusion

proteins were incubated with purified bovine G β γ protein (Calbiochem). Incubations were done in 800 μ l of binding buffer (200 mM NaCl, 10 mM EDTA, 10 mM Tris (pH 7.4), 0.1% Triton X-100, and protease inhibitor mixture set II) at 4 °C for 1 h. Then the beads were washed 5 times, and bound proteins were separated on 12% SDS-polyacrylamide gels. Bound G β γ was detected using a G β antibody (Santa Cruz Biotechnology) and a chemiluminescence kit (PerkinElmer Life Sciences). Finally, the relative amounts of G β γ were quantified by densitometry.

Immunofluorescence, Image Visualization, and Analysis

HEK293 cells were first fixed with 4% paraformaldehyde (0.1 M phosphate buffer (pH 7.4)) and were then permeabilized (0.3% Triton X-100) and blocked (10% normal horse serum). Subsequently, all night incubation with a monoclonal FLAG (Stratagene) and polyclonal hexahistidine antibodies (His-Tag, United States Biological) was carried out. Epitope visualization was performed by incubating the sample with two secondary antibodies conjugated to FITC and Cy3 (1:600; Jackson ImmunoResearch Laboratories). Finally, the cells were fitted with coverslips using Fluorescence Mounting Medium (Dako Cytomation). For quantitative analysis, cells were chosen randomly for imaging using a Nikon confocal microscope (TE2000, Nikon). Single stacks of optical sections in the z axis were acquired, and dual color immunofluorescent images were captured in simultaneous two-channel mode. Colocalization was studied by superimposing both color channels. The cross-correlation coefficient (r) between both fluorescence channels was measured using computer software (Metamorph, Universal Imaging Corp.) starting from separate immunoreactivity to GlyR-His and G β ₁-FLAG in the same cell (22). The theoretical maximum for r was 1 for identical images, and a value close to 0 implied a complete different localization of the labels. Subsequently, the obtained data were compiled, analyzed, and plotted.

Molecular Modeling

The GlyR model was constructed by homology using coordinates from the *Torpedo* nAChR at 4 Å resolution (23, 24) (PDB code 2BG9)

and acetylcholine-binding protein structure (PDB code 1UV6) (25) using the software Modeller (26, 27). The models were relaxed by energy minimization using a Conjugate Gradient protocol in the software GROMACS (28). To optimize the H-Bond net, the models were processed by the server REMO (29). Electrostatic surface potentials were calculated using APBS software (30). The individual charges were assigned using pdb2pqr software (31) with the AMBER force field (32). The final images were generated with Pymol (33).

Data Analysis

Statistical analyses were performed using ANOVA and are expressed as the mean \pm S.E.; values of $p < 0.05$ were considered statistically significant. For all the statistical analysis and plots, the Origin 6.0 (MicroCal) software was used. Normalized values were obtained by dividing the current amplitude obtained with time of GTPyS dialysis by the current at minute 1.

Results

Effects of G Protein Activation and Ethanol Sensitivity in Wild Type Glycine Receptor Subunits

GlyR subunit expression during development is highly regulated (4, 8, 9). Indeed, the α_2 GlyR is the main subunit during embryogenesis and early postnatal life, whereas α_1 GlyRs are present at adult stages. The presence of α_2 GlyRs in immature neurons and its absence in 2–3-week-old neurons has been consistently shown by different groups in both *in vitro* and *in vivo* preparations from rat and mouse, which has led to the study of functional properties of these GlyR subunits in their native configuration (4, 8). To investigate their sensitivity to G protein activation, we examined cultured spinal neurons at different developmental stages *in vitro* using intracellular applications of a non-hydrolyzable GTP analog (Fig. 1A). Previous reports using neuronal and recombinant α_1 GlyRs showed that the amplitude of the glycine-activated current was strongly enhanced after 15 min of intracellular dialysis with GTPyS, implying that G $\beta\gamma$ enhances GlyR activity (19). Interestingly, this modulation was only found in

older neurons ($63 \pm 13\%$, $n = 6$, 13–14 DIV) (Fig. 1A), indicating that the α_1 subunit is necessary for the G protein $\beta\gamma$ modulation. To test this further, we next studied G protein allosteric modulation using HEK 293 cells transfected with α_1 and α_2 GlyR isoforms. After 15 min of whole-cell recording in the presence of intracellular GTP γ S, only the glycine-evoked current elicited by α_1 GlyRs was strongly modulated ($77 \pm 13\%$, $n = 11$) (Fig. 1, C and E), suggesting that α_2 GlyRs lack some critical molecular characteristics for the G $\beta\gamma$ modulation despite their high sequence homology. To further characterize this modulation, we examined if G $\beta\gamma$ overexpression tonically modulated these two GlyRs, as described for Ca²⁺, GIRK (G protein-gated inwardly rectifying potassium) channels, and α_1 GlyRs (19, 34, 35). Previous studies using human α_1 GlyRs showed that the concentration-response relationship was shifted to the left after G $\beta\gamma$ dimers were coexpressed, reflected by a significant reduction in its EC₅₀ with respect to control cells (19). Similar to these results, rat α_1 GlyRs were tonically modulated by G $\beta\gamma$ overexpression, showing a decrease in their EC₅₀ from 41 ± 1 to 26 ± 2 μ M ($-34 \pm 6\%$ of tonic modulation) (Fig. 1B, supplemental Table 1). On the other hand, α_2 GlyRs did not show tonic modulation ($-4 \pm 7\%$). We next studied the ethanol sensitivity of these subunits using equipotent concentrations of glycine (EC₁₀) for each receptor and found that α_1 GlyRs were more sensitive to ethanol than α_2 subunits especially at low millimolar concentrations (Fig. 1, D–F). For example, the application of 100 mM ethanol potentiated the α_1 glycine-activated current in $54 \pm 7\%$ ($n = 8$), whereas the enhancement of the current in α_2 was only $9 \pm 3\%$ ($n = 7$). Thus, all this evidence indicates that these GlyR α isoforms are differentially modulated by G $\beta\gamma$ and ethanol despite their high homology. Recent studies have reported that G $\beta\gamma$ modulation is critical for ethanol effects on α_1 GlyRs (20). Therefore, it is possible to suggest that the allosteric action of ethanol on GlyRs is determined by differential interaction with G $\beta\gamma$ heterodimers.

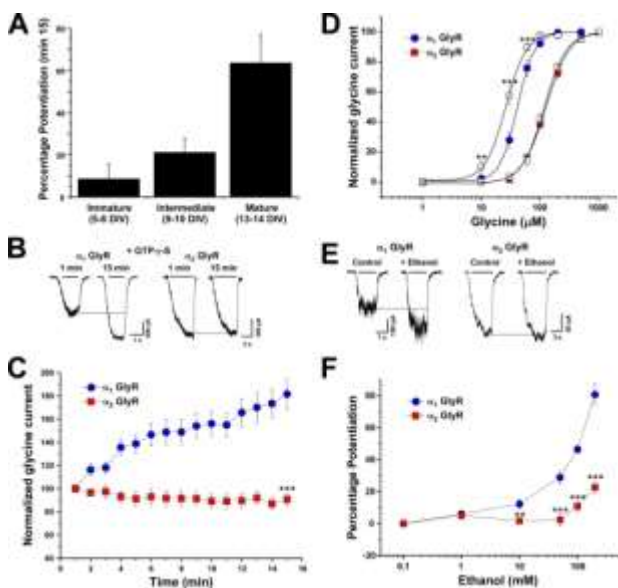


FIGURE 1. Effects of G protein activation and ethanol sensitivity of α_1 and α_2 GlyR subunits. *A*, the bar graph shows that only 13–14 DIV spinal neurons, which contain primarily α_1 GlyR subunits, are sensitive to G protein activation with GTP γ S. *B*, shown are current traces obtained in transfected HEK cells expressing wild type α_1 and α_2 GlyRs, recorded at 1 and 15 min of whole cell recording using intracellular GTP γ S. *C*, the graph summarizes the time course of the normalized glycine-evoked current elicited by α_1 and α_2 GlyRs during the dialysis with the non-hydrolyzable GTP analog. *D*, glycine concentration-response curves for α_1 and α_2 GlyRs in the absence (filled symbols) or presence of overexpressed G $\beta_1\gamma_2$ (open symbols). *E*, shown are examples of current traces in the presence or absence of 100 mM ethanol from wild type α_1 and α_2 GlyRs. *F*, shown are concentration-response curves for ethanol (1–200 mM) in α_1 and α_2 GlyRs using an equipotent glycine concentration (EC₁₀) for both receptors. Data are the means \pm S.E. from 9–15 cells. Differences were significant $p < 0.001$ (***), ANOVA.

Functional and Direct Protein Interaction between Glycine Receptor Subunits and G Protein $\beta\gamma$ Dimers

Because the discovery of the first effector protein for G $\beta\gamma$, an ever-increasing number of effectors have been reported (36, 37), including two members of the Cys-loop superfamily, GlyRs and nAChRs (19, 38). In both cases G protein $\beta\gamma$ subunits modulate these receptors in a phosphorylation-independent manner, generating an enhancement in the agonist-evoked current linked to an increased open channel probability. Additionally, *in vitro* experiments have shown a direct interaction between G $\beta\gamma$ and the large intracellular loop

of α_1 GlyRs and α_{3-4} nAChRs. Two basic amino acid motifs in the large intracellular loop of the human α_1 GlyR subunit are essential for G $\beta\gamma$ binding (³¹⁶RFRRK and ³⁸⁵KK), and these regions have been postulated to form an electropositive area that shapes the G $\beta\gamma$ interaction surface in a pentameric GlyR configuration. Supporting a causative role for G $\beta\gamma$ binding in ethanol potentiation of GlyRs, it was previously found that mutations in these sequences and reduction in the availability of free G $\beta\gamma$ altered the G $\beta\gamma$ binding and significantly attenuated the ethanol actions on recombinant and native GlyRs (20, 39).

To analyze the presence of these motifs within other GlyR subunits, the sequences of α_1 and α_2 GlyR intracellular loops were examined (Fig. 2A). The data showed that similar to the rat and human α_1 GlyR subunits (39), rat α_2 also presents these basic motifs. The expected structural homology in these two subunits is supported by structural modeling which shows that the intracellular regions important for G $\beta\gamma$ modulation are predicted to be α -helices, similar to those in the transmembrane regions (Fig. 2B) and the MA stretch of nAChR (23, 24). Furthermore, the electropositive surfaces for these motifs were conserved in α_1 and α_2 GlyRs. Thus, despite the absence of functional modulation, the data suggest that the α_2 GlyR isoform is capable of binding G $\beta\gamma$.

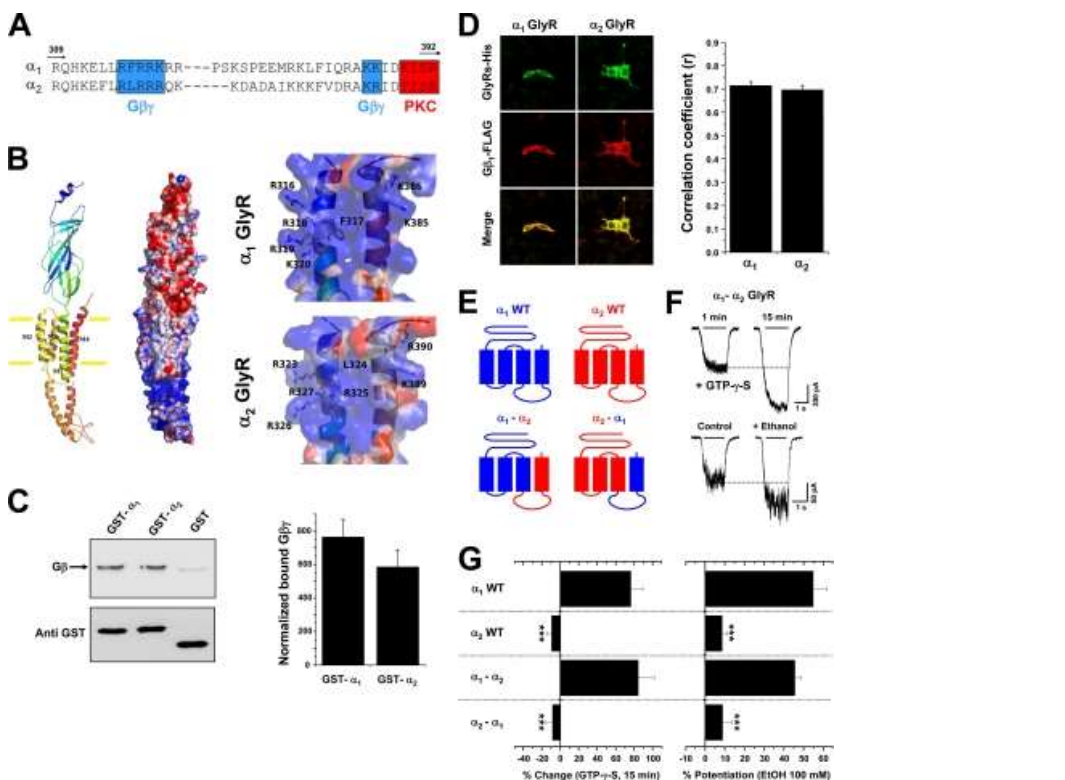


FIGURE 2. Functional protein interaction between G β γ and the α_2 GlyR TM3-4 loop. *A*, shown is partial primary sequence alignment between the TM3-4 loops of α_1 and α_2 GlyR subunits. Note that the critical basic residues for G β γ binding are conserved. *B*, shown are a ribbon diagram and electrostatic potential surface representations of a single GlyR α subunit modeled from the nAChR template. The *right panel* shows a detailed view of the motifs important for G β γ modulation. Negative and positive charges are in *red* and *blue*, respectively. *C*, G β binding to wild type GlyR subunits and total GST fusion protein amounts revealed using an antibody against GST. The *arrow* indicates G β bound to a polyclonal anti-G β antibody. The *graph* represents the relative amounts of bound G β normalized with their corresponding loaded amount of GST fusion protein. The values were obtained from five different experiments. *D*, HEK 293 cells transfected with G β_1 -FLAG, G γ_2 , and His-tagged α GlyRs were fixed and stained with antibodies against hexahistidine (*green*) and FLAG (*red*), which recognize tagged GlyRs and G β_1 , respectively. Images were merged to visualize colocalization. The graph summarizes the mean correlation coefficients (*r*) between GlyR subunits and G β_1 for each stained cell studied. *E*, shown is a schematic depiction of wild type and chimeric GlyRs used in this section. *F*, shown are current traces of chimeric α_1 - α_2 GlyRs-associated chloride currents in the presence of intracellular GTP γ S or after the application of 100 mM ethanol. *G*, the *bar graph* summarizes the effects of non-hydrolyzable GTP analog dialysis (15 min) and 100 mM ethanol on the glycine-evoked current. Statistical analyses were significant (***, *p* < 0.001, ANOVA, versus α_1 GlyRs).

To determine whether the α_2 GlyR intracellular loop is able to bind G $\beta\gamma$ proteins *in vitro*, we constructed GST fusion proteins encoding the TM3–4 loops. GST fusion proteins were first expressed and purified, and then *in vitro* binding assays were performed using purified G $\beta\gamma$ (Fig. 2C). In agreement with previous reports with human α_1 GlyRs (39), rat α_1 GlyR TM3–4 loop was able to bind G $\beta\gamma$ as compared with GST. The GST fusion protein containing the α_2 intracellular loop also binds G $\beta\gamma$, demonstrating the existence of protein-protein interactions. To further confirm these data in a cellular context, we performed double immunofluorescent analysis in HEK 293 cells transfected with α GlyRs and G $\beta_1\gamma_2$ subunits using hexahistidine and FLAG epitopes to identify the expressed GlyRs and G β_1 subunits, respectively. In agreement with the GST pulldown data, the cellular distribution of the GlyR isoforms and G $\beta\gamma$ dimers displayed a significant overlap in their expression patterns (Fig. 2D). The correlation analysis yielded high coefficient values, providing quantitative support for good colocalization between these GlyR isoforms and G $\beta\gamma$. Although the spatial resolution of confocal microscopy is limited, the significant colocalization of the GlyR isoforms and G $\beta\gamma$ is consistent with a direct interaction in a cellular context.

Altogether, these data demonstrate that the α_2 GlyR intracellular loop is able to interact with G $\beta\gamma$. Thus, we next designed a chimeric approach to test the presence of functional G $\beta\gamma$ modulation in this sequence. These chimeric GlyRs between α_1 and α_2 subunits were generated combining the coding region downstream from the TM3–4 loop of one specific subunit with the region upstream of the TM3 end of another subunit, giving GlyRs with exchanged intracellular loops plus TM4 (Fig. 2E). The analysis of agonist concentration-response curves shows that the α_1 - α_2 and α_2 - α_1 exchanges did not significantly modify the receptor physiology (supplemental Table 1). Next, we used intracellular dialysis with GTP γ S to evaluate the G protein $\beta\gamma$ modulation of these constructs. We found that the exchange of the TM3–4 loop of the α_1 subunit with the α_2 counterpart did not affect the G $\beta\gamma$ allosteric modulation (Fig. 2, F–G). For example, the GTP γ S-mediated current enhancement in the α_1 - α_2 GlyR was $85 \pm 17\%$ ($n = 7$), which was not significantly different from the wild type α_1 GlyR. On

the other hand, changing the TM3–4 loop of α_2 subunits with the corresponding α_1 region did not recover the G $\beta\gamma$ modulation despite the fact that the α_1 GlyR intracellular loop possesses all the molecular elements required for a functional modulation by the G protein heterodimer. Subsequently, the effect of 100 mM ethanol was studied on these GlyRs using an equipotent concentration of glycine for each construct. The α_1 - α_2 GlyR displayed a similar potentiation in comparison with the α_1 GlyR (Fig. 2G), whereas the α_2 - α_1 GlyRs remained insensitive to ethanol, in agreement with the results using GTP γ S.

Based on all these results, we conclude that changing the TM3–4 loop between the α_1 and α_2 receptor isoforms did not change the physiology, intracellular regulation, or ethanol pharmacology of the respective GlyRs. In addition, these results suggest that the absence of G $\beta\gamma$ functional modulation and low ethanol sensitivity displayed by α_2 GlyRs is due to the lack of molecular features that allow specific conformational changes after G $\beta\gamma$ binding, which finally generates the allosteric modulation of the ion channel.

Two Transmembrane Residues Are Critical for the G $\beta\gamma$ and Ethanol Allosteric Modulations of the GlyR α_1 Subunit

It is well accepted that the transmembrane regions of the LGIC superfamily members are critical for correct ion channel function and regulation. In the Cys-loop pentameric conformation, each subunit contributes four transmembrane domains to form the ion channel, with TM2 domains shaping the central ion pore (2). Using mutagenesis and electrophysiology, several studies have determined the importance of TM domains for GlyR function (2,–4). For example, residues Gly-254 and Ser-267 present in the TM2 domain of α_1 GlyRs contribute to single channel conductance and ethanol potentiation, respectively (10, 40, 41). Due to the potential role on the allosteric effects of ethanol, it is possible that residues in TM domains besides intracellular amino acids could explain the differential alcohol sensitivity displayed by these GlyR isoforms. To analyze this hypothesis, we first performed an alignment of the α GlyR subunits upstream of the TM3–4 loop,

focusing on the TM2–3 domains (Fig. 3A). These sequences displayed high homology profiles (>95%), with only two divergent residues at positions Gly-254 and Ser-296. Significantly, two critical residues involved in the ethanol and general anesthetic effects on GlyRs, Ser-267 and Ala-288 (40, 41), were fully conserved between α_1 and α_2 isoforms (Fig. 3A). Thus, these analyses suggest that these previously described residues cannot completely explain the differential ethanol sensitivity displayed by the GlyR isoforms, and we, therefore, focused our analyses toward the non-conserved TM amino acids. The primary sequences show that the α_1 GlyR, sensitive to G $\beta\gamma$ and ethanol, has Gly-254 in the TM2 and Ser-296 in the TM3, whereas the α_2 GlyR has two alanine residues in these positions (Fig. 3A). Despite these differences, our molecular modeling studies show that the α -helix conformation proposed for the TM domains was well conserved, supporting the experimental data that showed functional ligand-gated ion channels.

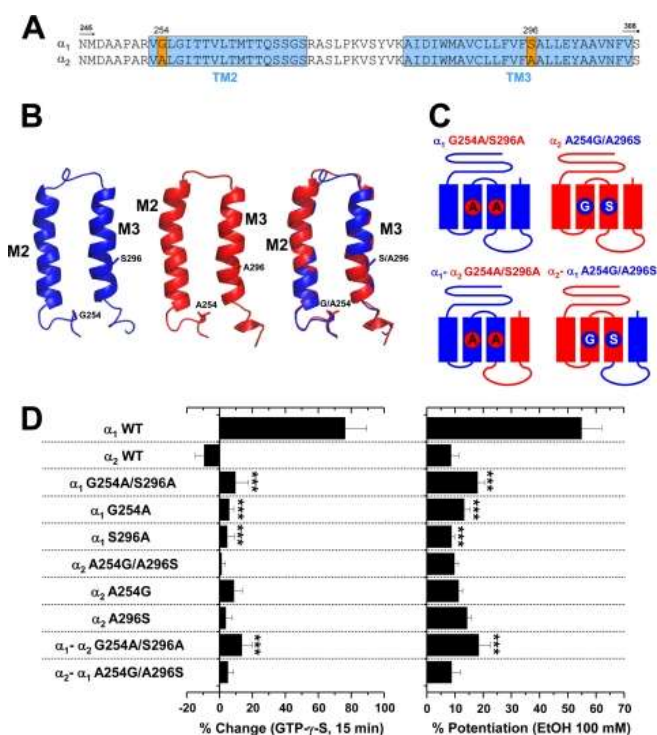


FIGURE 3.

Two transmembrane residues are critical for functional α_1 GlyR regulation by G $\beta\gamma$ and ethanol. A, shown is the primary sequence alignment between α_1 and α_2 GlyR subunits from the TM2 to TM3 region. The positions that correspond to Gly-254

and Ser-296 in wild type α_1 GlyRs were the only non-conserved residues and are highlighted in *orange*. *B*, shown are molecular representations of single α_1 (*blue*) and α_2 GlyR (*red*) TM regions. The superposition of both structures demonstrates that the overall α -helix structure is highly conserved. *C*, shown is a schematic representation of the chimeric and mutant GlyRs used to study the role of the non-conserved TM residues between α_1 and α_2 GlyRs. *D*, a *bar graph* summarizes the normalized glycine-evoked current after 15 min of dialysis with GTP γ S and the sensitivity to 100 mm ethanol of wild type, chimeric, and mutant GlyRs studied. Note that TM mutations in α_1 GlyRs abolished both G protein and ethanol effects, whereas reversal substitutions in α_2 GlyRs did not display any significant change. Differences were significant (***, $p < 0.001$, ANOVA) between α_1 GlyRs and all the TM mutants.

To investigate the importance of these non-conserved residues in TM2 and TM3, mutant and chimeric α_1 and α_2 GlyRs were generated to swap these residues between the constructs (Fig. 3C). Mutations G254A and S296A in the α_1 and α_1 - α_2 GlyRs significantly attenuated the effect of intracellular GTP γ S (Fig. 3D). For instance, the GTP γ S-mediated current enhancement in the α_1 G254A/S296A GlyR was only $10 \pm 8\%$ ($n = 6$). Application of 100 mm ethanol to the double-mutated α_1 GlyR also showed a significant decrease in the current potentiation ($18 \pm 2\%$ ($n = 7$)) (Fig. 3D). Interestingly, singly mutated α_1 GlyRs demonstrated that Gly-254 and Ser-296 can abolish G protein and ethanol actions, indicating that they also participate in G $\beta\gamma$ and ethanol modulations. Therefore, we should be able to recover G $\beta\gamma$ and ethanol modulation through reverse mutations in the α_2 GlyR, which we denominated A254G and A296S to conserve a nomenclature relative to α_1 GlyRs. Our electrophysiological analysis revealed that the double-mutated α_2 GlyR was not significantly modified, showing an unchanged apparent affinity for glycine (supplemental Table 1). Interestingly, the current elicited by the α_2 A254G/A296S GlyR was still insensitive to activation of G proteins and 100 mm ethanol, displaying a $3 \pm 2\%$ ($n = 5$) and a $10 \pm 2\%$ ($n = 7$) of potentiation, respectively (Fig. 3D). This behavior was conserved even when the A254G and A296S mutations were incorporated in the α_2 - α_1 GlyR, demonstrating that the presence of α_1 GlyR TM and intracellular sequences was not enough to recover the G $\beta\gamma$ and ethanol modulation of α_2 GlyRs. Therefore, we decided to explore regions upstream of the TM domains to determine the existence of other critical features that allow functional G protein regulation and high ethanol sensitivity.

Simultaneous Mutations in Transmembrane and Extracellular Residues within the α_2 GlyR Subunit Generate Ligand-gated Ion Channels Modulated by G $\beta\gamma$ with High Ethanol Sensitivity

The proposed current structure of the LGIC superfamily members comprises an extracellular domain with several β -sheets containing the neurotransmitter binding sites and other regions that allow coupling of agonist binding to channel opening (2,-4). Several electrophysiological and molecular modeling studies have postulated that loop 2 and loop 7 (the conserved "Cys-loop") are critical for receptor activation because they transfer energy of ligand binding to the transmembrane regions responsible for opening the ion channel (2,-4, 42,-44). It has been recently shown that two residues, Glu-53 and Asp-57, in loop 2 are critical for the activation mechanism of the α_1 GlyR (44). Interestingly, a specific mutation (A52S) within the same region of the α_1 GlyR has been previously linked to the *spasmodic* mice phenotype (45) and ethanol sensitivity (12, 18). However, the same residue has also been directly implicated in the generation of a pre-open flipped conformation of the ion channel that occurs after the binding of the agonist that precedes channel opening (46, 47). Taking into account this evidence, it is possible to postulate that the regions involved in the coupling of ligand binding to channel gating are responsible for the low allosteric actions of G $\beta\gamma$ and ethanol on the GlyR. To study this possibility, we examined loop 2, the Cys-loop, and the TM2-3 loops of α_1 and α_2 GlyR subunits (Fig. 4A). Like the TM domains, these α GlyR isoforms were highly conserved in these regions. Notably, the position that corresponds to Ala-52 within loop 2 of the α_1 GlyR was non-conserved due to the presence of a threonine residue within the α_2 GlyR isoform (Fig. 4A). Molecular modeling studies show that the conformation suggested for these domains were similar between the α subunits, showing a close proximity between the β -turns of the extracellular regions and the extracellular region of the ion channel TM2-3 loop (2, 44) (Fig. 4B). However, the α_2 GlyR loop 2 displays an extended β -strand structure that is also observed when the mutation A52T was introduced in the α_1 GlyR. Thus, we investigated the importance of this position for the allosteric actions of G $\beta\gamma$ and

ethanol on α_1 and α_2 GlyRs (Fig. 4C). As previously described (12, 17, 48), the A52T mutation significantly impaired the apparent affinity for glycine and ethanol sensitivity of the α_1 subunit. Additionally, it also attenuated the G protein activation (Fig. 4, C–G). For instance, the GTP γ S-mediated current enhancement in the α_1 A52T GlyR was only $13 \pm 2\%$ ($n = 6$), whereas the ethanol potentiation induced by 100 mM was $16 \pm 2\%$ ($n = 6$). The results suggest that this single amino acid is a key element serving to explain the resistance of the α_2 GlyRs to G $\beta\gamma$ and ethanol modulations. To explore this idea, we generated the reverse T52A mutation within the wild type α_2 GlyR sequence, which we denominated as T52A in the α_2 GlyR to conserve the nomenclature relative to α_1 GlyRs. Contrary to the results obtained with the α_1 A52T mutant, the analysis of the concentration-response curve of the reverse T52A in α_2 showed a significant left-shift displacement in the apparent affinity for glycine, as previously described (48) (supplemental Table 1). Despite this change, this substitution did not restore the G protein modulation or the ethanol sensitivity (Fig. 4, E–G). However, this result is consistent with the absence of the critical TM elements (Gly-254 and Ser-296) for the G protein and alcohol regulation. Thus, these results strongly suggest that the full recovery of G $\beta\gamma$ and ethanol modulation in α_2 GlyRs could be achieved through the simultaneous TM plus loop 2 reversal mutations. In agreement with this, the triple-mutated α_2 T52A/A254G/A296S GlyR displays high G protein modulation, showing a $87 \pm 7\%$ ($n = 6$) enhancement in the glycine-activated current after intracellular dialysis with GTP γ S (Fig. 4, E–G). Noteworthy, these exchanges also generated a GlyR sensitive to pharmacological ethanol concentrations, displaying a $57 \pm 7\%$ ($n = 6$) of current potentiation with 100 mM ethanol (Fig. 4, D–G). This phenomenon was also reproduced when these three substitutions were included in the α_2 - α_1 GlyR, demonstrating that the ethanol and G $\beta\gamma$ modulation of α_2 GlyRs are controlled by contributions of TM2–3 and loop 2 that are unique in the α_1 GlyR (Fig. 4G).

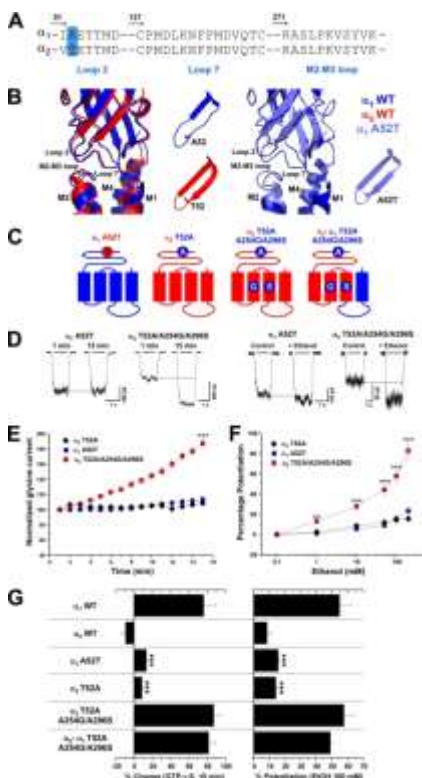


FIGURE 4. Selective substitutions within the extracellular loop 2 and transmembrane domains of α_2 GlyRs generate receptors functionally modulated by $G\beta\gamma$ with high ethanol sensitivity. *A*, sequence alignments of loops 2, 7, and TM2–3 in α_1 and α_2 GlyRs are shown. The position Ala-52 in α_1 GlyRs is highlighted as an important non-conserved residue. *B*, shown are ribbon diagram representations of a single α_1 GlyR subunit (*blue*) superposed with α_2 (*red*) or α_1 A52T mutant (*cyan*). The *two insets* represent a detailed view of loop 2. Note that wild type α_2 or α_1 A52T GlyRs displays an extension of the β -strain into the β -turn structure. *C*, shown are schematic representations of the mutant GlyRs used to study the role of the extracellular loop 2. *D*, shown are examples of whole-cell recordings from α_1 A52T and α_2 T52A/A254G/A296S GlyRs in the presence of intracellular GTP γ S or during the application of 100 mm ethanol. *E*, shown is the time course of the G protein activation effect on the normalized glycine-evoked currents elicited by α_1 A52T, α_2 T52A, and α_2 T52A/A254G/A296S GlyRs. *F*, shown are concentration-response curves to ethanol (1–200 mm) in α_1 A52T, α_2 T52A, and α_2 T52A/A254G/A296S GlyRs using an equipotent glycine concentration (EC_{10}). *G*, the plot summarizes the normalized glycine-evoked current after 15 min of dialysis with GTP γ S, and the sensitivity to 100 mm ethanol of the mutants was studied. Note that only the simultaneous loop 2 and TM residue substitutions in α_2 GlyRs were capable of generating GlyRs sensitive to G protein and ethanol, whereas only a single loop 2 mutation in α_1 GlyRs was enough to abolish G

protein and ethanol sensitivity. Differences were significant (**, $p < 0.01$; ***, $p < 0.001$, ANOVA).

To confirm the high ethanol sensitivity at the single channel level, we performed outside-out recordings from membranes expressing wild type α_1 , α_2 , and the α_2 T52A/A254G/A296S GlyRs. Application of 10 mM ethanol strongly modulated wild type α_1 GlyRs, producing a significant enhancement of the open-channel probability ($144 \pm 19\%$ above control, $n = 5$) without changes in the main conductance (92 ± 2 versus 93 ± 2 picosiemens in the presence of ethanol) (Fig. 5, A and B). On the other hand, α_2 GlyRs were not significantly affected by ethanol ($7 \pm 2\%$, $n = 5$), in accordance with the results obtained by using the whole-cell configuration. Both ion channels displayed their previously reported features, with a higher main conductance (122 ± 4 picosiemens) and long openings for α_2 GlyRs versus the presence of different levels of subconductance and long opening bursts for α_1 GlyRs (Fig. 5, A and B, supplemental Table 2) (3, 10–11, 49). Interestingly, the α_2 T52A/A254G/A296S GlyRs displayed a single channel profile similar to wild type α_1 GlyRs, exhibiting similar open time distribution profiles with a main-channel conductance of 87 ± 2 picosiemens (Fig. 5, A and B, supplemental Table 2). Moreover, these GlyRs fully recovered the sensitivity to ethanol, displaying an important enhancement of the open-channel probability ($153 \pm 44\%$, $n = 5$) that was not significantly different from wild type α_1 GlyRs. Further analysis indicated that both ethanol-sensitive receptors displayed a significant increase in the mean open time during ethanol application, whereas the open time for α_2 GlyRs remained unchanged (Fig. 5, A–C, supplemental Table 2). Nevertheless, it is interesting to note that the general activity profile of the α_2 T52A/A254G/A296S GlyRs was not absolutely equivalent to the wild type α_1 GlyRs, suggesting that only the G protein and ethanol sensitivity rather than the overall ion channel function was specifically influenced by these three mutations (Fig. 5A).

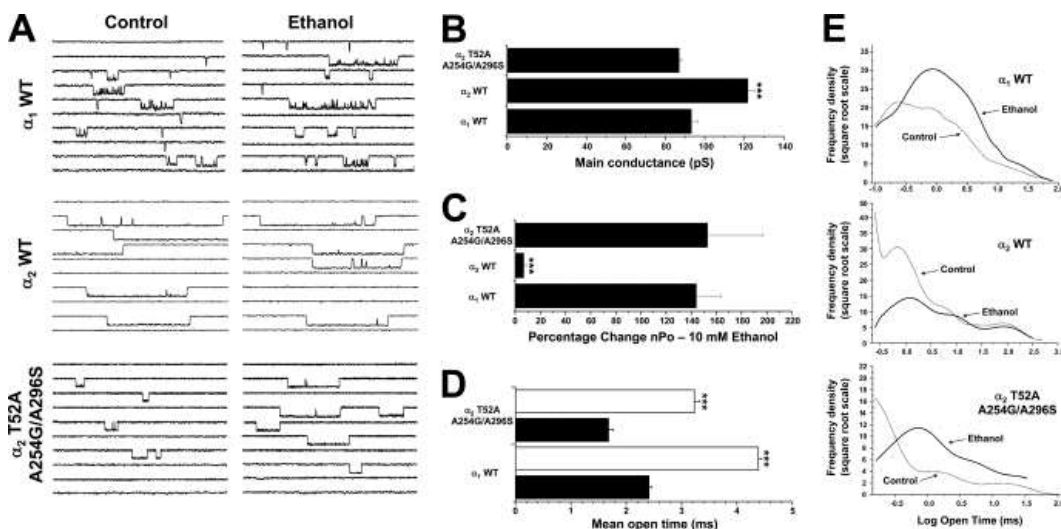


FIGURE 5. Ethanol effects on single-channel activity in the mutant α_2 T52A/A254G/A296S and wild type α GlyRs. *A*, shown are single-channel recordings from wild type α_1 , α_2 , and mutant α_2 T52A/A254G/A296S GlyRs before and after the application of 10 mM ethanol. Scale bar, 5 pA, 10 ms. *B*, the graph shows that the wild type α_2 GlyR mean conductance was modified by the TM substitutions in the α_2 T52A/A254G/A296S mutant. *C*, the bar graph summarizes the percentage change of open probability during application of 10 mM ethanol. Differences between wild type α_2 and mutant α_2 T52A/A254G/A296S were significant. *D*, the graph shows that the mean open time of both wild type α_1 and mutant α_2 T52A/A254G/A296S were significantly increased by ethanol to a similar extent. *E*, the histograms summarize the frequency plots for open times in each GlyR in the absence or presence of ethanol. Differences were significant (***, $p < 0.001$, ANOVA).

Altogether we identified key residues in extracellular and TM domains that fully explain the differential G $\beta\gamma$ and ethanol sensitivity of the α_1 and α_2 GlyRs. In addition, because extracellular, TM, and intracellular elements of the GlyR isoforms at the same time modulates the functional G $\beta\gamma$ modulation and ethanol sensitivity, it is possible to suggest the existence of a direct relationship between ethanol sensitivity and G $\beta\gamma$ modulation. In agreement with our previous evidence (20), we found a highly significant correlation between the sensitivity of the receptors to 100 mM ethanol and G protein activation ($r^2 = 0.9664$, $p < 0.0001$) plotting the wild type, chimeric, and mutated GlyRs (supplemental Fig. 1). Thus, these data provide additional evidence indicating that G $\beta\gamma$ signaling participates in the differential ethanol modulation of these GlyR isoforms.

Discussion

The results shown here and others that we previously described (20) allow us to identify the molecular elements that explain the differential ethanol sensitivity of two receptors that belong to the Cys-loop superfamily based on the selective intracellular modulation through G protein $\beta\gamma$ subunits. Interestingly, these requirements are found along the receptor, suggesting that the G $\beta\gamma$ and ethanol sensitivity lies on a series of subtle changes impacting the channel structure. The first of these elements consists of a direct interaction of the G $\beta\gamma$ dimer with the receptor through basic residues in the TM3–4 intracellular loop (20, 39). The data showed that α_1 and α_2 GlyRs bind G $\beta\gamma$, but only the α_1 GlyR conformation allowed an effective conversion of G $\beta\gamma$ binding into functional allosteric modulation. Two other residues within the α_1 GlyR TM domains were identified as key elements for a transmembrane configuration that will allow ion channel conformational changes after G $\beta\gamma$ binding. The data showed that the presence of Gly-254 in TM2 and Ser-296 in TM3 in addition to G $\beta\gamma$ binding was not enough to facilitate channel opening in α_2 GlyRs, thus, directing our attention into sites that drive the coupling of agonist binding to channel gating described for the Cys-loop ion channels. In agreement with this idea, we determined that an extracellular residue present in the loop 2 of α_1 GlyRs (Ala-52) is another critical feature for high sensitivity to G $\beta\gamma$ and ethanol. Interestingly, this particular residue has been postulated as a key factor for the GlyR function based on studies using the α_1 GlyR A52S mutation present in the *spasmodic* mouse, which is the amino acid present in the wild type α_2 GlyRs at that position (12, 17, 45). The functional characterization of this mutant showed low glycine apparent affinity, unchanged agonist binding, low ethanol sensitivity, and slow synaptic kinetics (45, 50). To explain these changes, recent single channel analysis postulated a mechanism in which the A52S mutation in the human α_1 GlyR impairs the transition between a resting closed state and a pre-opened closed state (denominated “flipped” state) of the glycine-bound GlyR, without changes in the final transition from the flipped state to the opened state (*i.e.* channel “gating”) (47, 51). Particularly, Plested *et al.* (47) postulated that the most plausible effect of the A52S mutation on the receptor function was a 100-fold reduction on glycine affinity for the

flipped conformation. Because Ala-52 is in a region thought to be involved in the transduction of agonist binding to channel gating (2, 43–44, 46, 47), its mutation appears to affect the conformational changes leading to channel opening. Furthermore, the affinity of the agonist for the flipped conformation is a key determinant to explain the differences between full and partial agonists (51). Considering all this evidence, we propose that G $\beta\gamma$ and ethanol modulations also require a highly efficient transition toward the flipped conformation, which is favored in Ala-52- α_1 but possibly impaired in the Thr-52- α_2 GlyRs. Interestingly, molecular modeling shows that this residue extends the β -strand into the loop 2 structure, giving rigidity to this region and possibly affecting interactions with neighboring residues.

Thus, all the previous findings (20, 47, 51) and the present results allow us to propose a model that explains the differential G $\beta\gamma$ and ethanol sensitivity of α_1 and α_2 GlyRs using an overall view of the ion channel structure (Fig. 6). Remarkably, these results show for the first time that the ethanol sensitivity of a Cys-loop LGIC member can be recovered by specific mutations that are not related to a direct binding of alcohol within the ion channel structure. Also, the data suggest that transmembrane conformational changes within the ion channel structure after G $\beta\gamma$ binding and the isomerization rate to the pre-open flipped state are core elements to explain the differential ethanol sensitivity of these two GlyR isoforms. It is important to note that our study postulates the pre-open flipped conformation as a requirement for the optimal intracellular regulation and ethanol sensitivity of the Cys-loop superfamily, which is complementary with the key role that this transition has to explain the partial agonism within the Cys-loop superfamily (51). Furthermore, these data confirm the critical role of G $\beta\gamma$ signaling as an important determinant for the ethanol sensitivity of the GlyRs, which also might be important to explain the diverse effects of ethanol on γ -aminobutyric acid receptors (52,–54). Because several properties of the Cys-loop ion channels can be modified by the presence or absence of specific subunits in the pentameric structure, this study also raises the possibility that different subunit combinations within the Cys-loop family members could give receptors with differential G $\beta\gamma$ sensitivities based on specific transmembrane configurations and flipping rates, which will display

highly variable ethanol sensitivities depending on signal transduction states. In summary, these data provide support for the hypothesis that a main determinant for some Cys-loop ion channels with different ethanol sensitivities arises from a selective G $\beta\gamma$ modulation. Thus, this mechanism provides a novel mechanism of action regarding the LGIC superfamily regulation by alcohol, which could help to understand the complex nature of alcohol effects on the human nervous system.

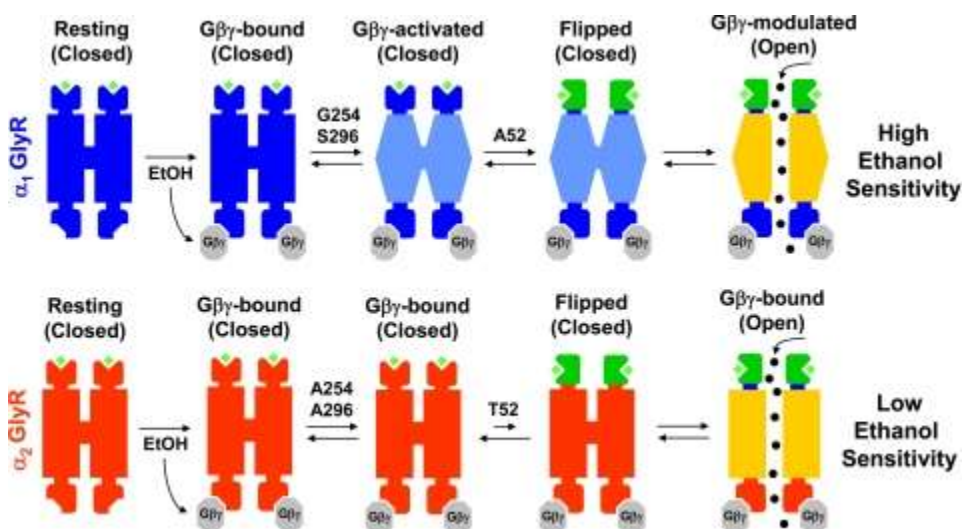


FIGURE 6. Molecular requirements for G $\beta\gamma$ and ethanol modulations of α_1

and α_2 GlyRs. In a resting state with glycine bound, G protein activation or pharmacological ethanol concentrations increase free G $\beta\gamma$ dimer availability, which subsequently interacts with α_1 and α_2 GlyRs through conserved basic residues within the TM3–4 loop. Intracellular G $\beta\gamma$ binding induces a conformational change in the TM domains, generating a GlyR with a G $\beta\gamma$ -activated conformation. The presence of the pivotal residues Gly-254 and Ser-296 in α_1 GlyRs allow reaching this configuration. Previous to channel opening, the receptor should change its conformation toward a pre-opened or flipped state, which is believed to depend on residues that control the coupling of agonist binding to channel opening. The Ala-52 in α_1 GlyRs has been previously shown to be critical for a facilitated transition from resting to flipped states, which is also a requirement for a functional G $\beta\gamma$ modulation. Thus, only the GlyRs with a G $\beta\gamma$ -activated TM configuration and suitable flipping rates can be modulated by G $\beta\gamma$, resulting in receptors with high ethanol sensitivity.

Acknowledgments: We thank Lauren Aguayo for technical assistance. We also thank Dr. Bryan McCool (Wake Forest University) for providing the plasmids encoding wild type GlyR subunits.

*This work was supported, in whole or in part, by National Institute on Alcohol Abuse and Alcoholism Grant RO1 AA15150 (to L. G. A.). This work was also supported by Comision Nacional de Investigacion Cientifica y Tecnologica Grant AT-4040102 (to G. E. Y.).

The on-line version of this article (available at <http://www.jbc.org>) contains supplemental Tables 1 and 2 and Fig. 1.

The abbreviations used are:

GlyR glycine receptor
LGIC ligand-gated ion channel
nAChR nicotinic acetylcholine receptor
GTP γ S guanosine 5'-O-(3-thiotriphosphate)
ANOVA analysis of variance
TM transmembrane domain.

References

1. Kandel E. R., Schwartz J. H., Jessell T. M. (2000) Principles of Neural Science, 4th Ed., pp. 175–317, McGraw-Hill Medical
2. Sine S. M., Engel A. G. (2006) *Nature* 440, 448–455
3. Lynch J. W. (2004) *Physiol. Rev.* 84, 1051–1095
4. Legendre P. (2001) *Cell. Mol. Life Sci.* 58, 760–793
5. Laube B., Maksay G., Schemm R., Betz H. (2002) *Trends Pharmacol. Sci.* 23, 519–527
6. Harvey R. J., Depner U. B., Wässle H., Ahmadi S., Heindl C., Reinold H., Smart T. G., Harvey K., Schütz B., Abo-Salem O. M., Zimmer A., Poisbeau P., Welzl H., Wolfer D. P., Betz H., Zeilhofer H. U., Müller U. (2004) *Science* 304, 884–887
7. Sebe J. Y., van Brederode J. F., Berger A. J. (2006) *J. Neurophysiol.* 96, 391–403
8. Aguayo L. G., van Zundert B., Tapia J. C., Carrasco M. A., Alvarez F. J. (2004) *Brain Res. Brain Res. Rev.* 47, 33–45
9. Malosio M. L., Marquèze-Pouey B., Kuhse J., Betz H. (1991) *EMBO J.* 10, 2401–2409
10. Bormann J., Rundström N., Betz H., Langosch D. (1993) *EMBO J.* 12, 3729–3737
11. Mangin J. M., Baloul M., Prado, De Carvalho L., Rogister B., Rigo J. M., Legendre P. (2003) *J. Physiol.* 553, 369–386
12. Mascia M. P., Mihic S. J., Valenzuela C. F., Schofield P. R., Harris R. A. (1996) *Mol. Pharmacol.* 50, 402–406

13. Maksay G., Laube B., Betz H. (2001) *Neuropharmacology* 41, 369–376
14. Miller P. S., Da Silva H. M., Smart T. G. (2005) *J. Biol. Chem.* 280, 37877–37884
15. Tapia J. C., Aguayo L. G. (1998) *Synapse* 28, 185–194
16. Eggers E. D., O'Brien J. A., Berger A. J. (2000) *J. Neurophysiol.* 84, 2409–2416
17. Perkins D. I., Trudell J. R., Crawford D. K., Alkana R. L., Davies D. L. (2008) *J. Neurochem.* 106, 1337–1349
18. Crawford D. K., Trudell J. R., Bertaccini E. J., Li K., Davies D. L., Alkana R. L. (2007) *J. Neurochem.* 102, 2097–20109
19. Yevenes G. E., Peoples R. W., Tapia J. C., Parodi J., Soto X., Olate J., Aguayo L. G. (2003) *Nat. Neurosci.* 6, 819–824
20. Yevenes G. E., Moraga-Cid G., Peoples R. W., Schmalzing G., Aguayo L. G. (2008) *Proc. Natl. Acad. Sci. U.S.A.* 105, 20523–20528
21. Ren H., Honse Y., Karp B. J., Lipsky R. H., Peoples R. W. (2003) *J. Biol. Chem.* 278, 276–283
22. Agnati L. F., Fuxe K., Torvinen M., Genedani S., Franco R., Watson S., Nussdorfer G. G., Leo G., Guidolin D. (2005) *J. Histochem. Cytochem.* 53, 941–953
23. Miyazawa A., Fujiyoshi Y., Unwin N. (2003) *Nature* 423, 949–955
24. Unwin N. (2005) *J. Mol. Biol.* 346, 967–989
25. Celie P. H., van Rossum-Fikkert S. E., van Dijk W. J., Brejc K., Smit A. B., Sixma T. K. (2004) *Neuron* 41, 907–914
26. Eswar N., Webb B., Marti-Renom M. A., Madhusudhan M. S., Eramian D., Shen M. Y., Pieper U., Sali A. (2006) *Current Protocols in Bioinformatics*, Chapter 5: Unit 5.6, Wiley Interscience, John Wiley & Sons, Inc., New York
27. Martí-Renom M. A., Stuart A. C., Fiser A., Sánchez R., Melo F., Sali A. (2000) *Annu. Rev. Biophys. Biomol. Struct.* 29, 291–325
28. Hess B., Kutzner C., van der Spoel D., Lindahl E. (2008) *J. Chem. Theory Comput.* 4, 435–447
29. Li Y., Zhang Y. (2009) *Proteins* 76, 665–676
30. Baker N. A., Sept D., Joseph S., Holst M. J., McCammon J. A. (2001) *Proc. Natl. Acad. Sci.* 98, 10037–10041
31. Dolinsky T. J., Nielsen J. E., McCammon J. A., Baker N. A. (2004) *Nucleic Acids Res.* 32, W665–W667
32. Cornell W. D., Cieplak P., Bayly C. I., Gould I. R., Merz K. M., Ferguson D. M., Spellmeyer D. C., Fox T., Caldwell J. W., Kollman P. (1995) *J. Am. Chem. Soc.* 117, 5179–5197
33. DeLano W. L. (2002) *The PyMOL Molecular Graphics System*, DeLano Scientific LLC, San Carlos, CA
34. Ikeda S. R. (1996) *Nature* 380, 255–258

35. Ruiz-Velasco V., Ikeda S. R. (2001) *J. Physiol.* 537, 679–692
36. Clapham D. E., Neer E. J. (1997) *Annu. Rev. Pharmacol. Toxicol.* 37, 167–203
37. Hamm H. E. (1998) *J. Biol. Chem.* 273, 669–672
38. Fischer H., Liu D. M., Lee A., Harries J. C., Adams D. J. (2005) *J. Neurosci.* 25, 3571–3577
39. Yevenes G. E., Moraga-Cid G., Guzmán L., Haeger S., Oliveira L., Olate J., Schmalzing G., Aguayo L. G. (2006) *J. Biol. Chem.* 281, 39300–39307
40. Mihic S. J., Ye Q., Wick M. J., Koltchine V. V., Krasowski M. D., Finn S. E., Mascia M. P., Valenzuela C. F., Hanson K. K., Greenblatt E. P., Harris R. A., Harrison N. L. (1997) *Nature* 389, 385–389
41. Ye Q., Koltchine V. V., Mihic S. J., Mascia M. P., Wick M. J., Finn S. E., Harrison N. L., Harris R. A. (1998) *J. Biol. Chem.* 273, 3314–3319
42. Absalom N. L., Lewis T. M., Schofield P. R. (2004) *Exp. Physiol.* 89, 145–153
43. Absalom N. L., Lewis T. M., Kaplan W., Pierce K. D., Schofield P. R. (2003) *J. Biol. Chem.* 278, 50151–50157
44. Crawford D. K., Perkins D. I., Trudell J. R., Bertaccini E. J., Davies D. L., Alkana R. L. (2008) *J. Biol. Chem.* 283, 27698–27706
45. Ryan S. G., Buckwalter M. S., Lynch J. W., Handford C. A., Segura L., Shiang R., Wasmuth J. J., Camper S. A., Schofield P., O'Connell P. A. (1994) *Nat. Genet.* 7, 131–135
46. Pless S. A., Lynch J. W. (2009) *J. Biol. Chem.* 284, 27370–27376
47. Plested A. J., Groot-Kormelink P. J., Colquhoun D., Sivilotti L. G. (2007) *J. Physiol.* 581, 51–73
48. Miller P. S., Harvey R. J., Smart T. G. (2004) *Br. J. Pharmacol.* 143, 19–26
49. Beato M., Groot-Kormelink P. J., Colquhoun D., Sivilotti L. G. (2002) *J. Gen. Physiol.* 119, 443–466
50. Graham B. A., Schofield P. R., Sah P., Margrie T. W., Callister R. J. (2006) *J. Neurosci.* 26, 4880–4890
51. Lape R., Colquhoun D., Sivilotti L. G. (2008) *Nature* 454, 722–727
52. Aguayo L. G., Peoples R. W., Yeh H. H., Yevenes G. E. (2002) *Curr. Top. Med. Chem.* 2, 869–885
53. Wallner M., Hancher H. J., Olsen R. W. (2006) *Pharmacol. Ther.* 112, 513–528
54. Qi Z. H., Song M., Wallace M. J., Wang D., Newton P. M., McMahon T., Chou W. H., Zhang C., Shokat K. M., Messing R. O. (2007) *J. Biol. Chem.* 282, 33052–33063

About the Authors

- Gonzalo E. Yevenes, contributed equally to this work
Laboratory of Neurophysiology, Department of Physiology, University of Concepción, Concepción, Chile
Present address: Institute of Pharmacology and Toxicology, University of Zurich, Winterthurerstrasse 190, CH-8057, Zurich, Switzerland.
- Gustavo Moraga-Cid, contributed equally to this work
Laboratory of Neurophysiology, Department of Physiology, University of Concepción, Concepción, Chile
- Ariel Avila
Laboratory of Neurophysiology, Department of Physiology, University of Concepción, Concepción, Chile
- Leonardo Guzman
Laboratory of Neurophysiology, Department of Physiology, University of Concepción, Concepción, Chile
- Maximiliano Figueroa
Department of Biochemistry and Molecular Biology, University of Concepción, Concepción, Chile
- Robert W. Peoples
Department of Biomedical Sciences, Marquette University, Milwaukee, WI
- Luis G. Aguayo
Laboratory of Neurophysiology, Department of Physiology, University of Concepción, Concepción, Chile
To whom correspondence should be addressed: Dept. of Physiology, University of Concepción, P. O. Box 160-C, Concepción, Chile., Tel.: Phone: 56-41-203380; Fax: 56-41-245975; E-mail: laguayo@udec.cl